A NEW APPROACH TO TOP-PAIR PRODUCTION AT NNLO* **

René Ángeles-Martínez

H. Niewodniczański Institute of Nuclear Physics, Polish Academy of Sciences
Radzikowskiego 152, 31-342 Kraków, Poland

(Received November 6, 2017)

We report progress on a new approach to calculate top-pair production cross sections at NNLO. This consists in combining the slicing method with the soft collinear effective theory. The necessary matrix elements already exist in the literature except for the soft function at NNLO. We describe a strategy to evaluate this function numerically, and make a robust validation against the renormalisation group and our analytic results.

DOI:10.5506/APhysPolB.48.2267

1. Introduction

The top-pair ($t\bar{t}$) production is relevant for searches of a new physics at the LHC [1]. With the experiment providing highly precise data, the community is motivated to strengthen the current theoretical understanding of this process. Some important aspects that are currently being studied are the top mass definition, its decay modelling and the perturbative QCD corrections. Here, we focus on the latter. At the moment, only one group has calculated the full total and differential QCD corrections at NNLO [2–4] and other groups have reported partial results [5–7] that agree at the level of the total cross section. In addition, there are various approximate results at this order, see Refs. [8–13].

In these proceedings, we report progress on a new approach to evaluate a wide-range of differential cross sections at NNLO. We have the two-fold motivation of providing a full independent test of such cross sections and of developing an approach that can be applied to other processes at high orders, *e.g.* $gg \to H$ at N^{3}LO. The approach brings together various strategies tested in the literature:

* Presented at the XLI International Conference of Theoretical Physics "Matter to the Deepest", Podlesice, Poland, September 3–8, 2017.

** Work in collaboration with Michał Czakon and Sebastian Sapeta.

1. Firstly, we use the key observation of the slicing method [7, 14] that a cross section $\sigma_{t\bar{t}}^{\mathrm{NNLO}}$ integrated over the transverse momentum of the $t\bar{t}$ pair, q_{T}, can be written as

$$\sigma_{t\bar{t}}^{\mathrm{NNLO}} = \int\limits_{q_{\mathrm{T}}<q_{\mathrm{Tcut}}} \mathrm{d}q_{\mathrm{T}} \frac{\mathrm{d}\sigma_{t\bar{t}}^{\mathrm{NNLO}}}{\mathrm{d}q_{\mathrm{T}}} + \int\limits_{q_{\mathrm{T}}>q_{\mathrm{Tcut}}} \mathrm{d}q_{\mathrm{T}} \frac{\mathrm{d}\sigma_{t\bar{t}}^{\mathrm{NLO+jet}}}{\mathrm{d}q_{\mathrm{T}}} . \tag{1}$$

   The second term on the right-hand side is well-known, see for example [15, 16].

2. Secondly, to calculate the small-q_{T} region ($q_{\mathrm{T}} < q_{\mathrm{Tcut}}$), we adopt Soft Collinear Effective Theory (SCET), which has been applied to the same process at NLO [17]. All the relevant SCET operators except the soft function are know up to NNLO.

3. Finally, the graphs contributing to the soft function at NNLO have a common structure that can be algorithmically evaluated using a numerical approach.

In the following sections, we discuss points 2 and 3 from this list and in Section 4, we validate our algorithm by cross-checking against the contributions involving fermions: a part of the NNLO soft function that, by itself, can be compared against the SCET renormalisation group and that we have been able to evaluate analytically.

2. SCET for the small-q_{T} region

Let us denote by p_1 and p_2 the momenta of the incoming partons that interact to produce a pair of top quarks with momenta p_t and $p_{\bar{t}}$, plus additional partonic radiation X, *i.e.* we are interested in the process

$$q(p_1) + \bar{q}(q_2) \to t(p_t) + \bar{t}(p_{\bar{t}}) + X\,. \tag{2}$$

The SCET framework ascertains [17], first, that when the momentum of the top pair $q = p_t + p_{\bar{t}}$ satisfies

$$\Lambda_{\mathrm{QCD}} \ll q_{\mathrm{T}}^2 \ll q^2, m_t^2, (p_1+p_2)^2, (p_1-p_t)^2 - m_t^2, (p_1-p_{\bar{t}})^2 - m_t^2\,, \tag{3}$$

the states X, which are not power suppressed[1] have the momentum $(k^{\pm}, k^{\mp}, k_{\mathrm{T}}^{\mu})$ that is either hard $k \sim (1,1,1)$, soft $k \sim (\lambda,\lambda,\lambda)$ or collinear $k \sim (\lambda^2, 1, \lambda)$, where $\lambda = \Lambda/q_{\mathrm{T}}$ and, second, that the cross section can be written as the convolution of hard ($\boldsymbol{H}_{i\bar{i}}$), soft ($\boldsymbol{S}_{i\bar{i}}$) and beam ($B_i$) functions

[1] $\Lambda^2/q_{\mathrm{T}}^2$ or Λ^2/q^2.

that, respectively, describe the physics of these regions. Schematically, this can be written as

$$\frac{\mathrm{d}\sigma_{t\bar{t}}}{\mathrm{d}q_{\mathrm{T}}^2\,\mathrm{d}y\,\mathrm{d}q^2\,\mathrm{d}\cos\theta} = \sum_X \sum_{i=q,\bar{q},g} B_i(\xi_1, x_{\mathrm{T}}, \mu) \otimes B_{\bar{i}}(\xi_2, x_{\mathrm{T}}, \mu) \otimes \mathrm{Tr}\left[\boldsymbol{H}_{i\bar{i}}\left(q^2, m, v_t, \mu\right) \otimes \boldsymbol{S}_{i\bar{i}}(x_{\mathrm{T}}, v_t, \mu)\right] , \quad (4)$$

where μ is the factorisation scale, the sum over i runs over the possible production channels, and the convolution should be understood over the longitudinal factions ξ_i and the transverse coordinates $x_\perp$. The kinematical variables y and v_t are defined in the $t\bar{t}$ rest frame, y is the rapidity of $t\bar{t}$ pair and

$$p_t = m_t\left(1-\beta^2\right)^{-1}(1, \beta v_t)\,, \qquad v_t = \beta\,(\cos\theta, \sin\theta\,\hat{n}_{\mathrm{T}})\ , \quad (5)$$

where $\beta = \sqrt{1-4m_t^2/q^2}$ is the velocity of p_t. We refer the reader to Refs. [17, 18] for a detailed presentation of this expression.

In SCET, the soft, hard and beam functions have perturbative expansions, each of which is potentially simpler than the expression for the complete cross section. In the case of Eq. (4), the hard function and the process-independent beam functions [18, 19] are known up to NNLO but the soft function is only known up to NLO [17].

3. Integration strategy of the soft function at NNLO

We work in the momentum space, $\boldsymbol{S}_{i\bar{i}}(q'_{\mathrm{T}}, v_t, \mu)$, where the soft function amounts to a product of Wilson lines with soft emissions having a fixed total transfer momenta, q'_{T}. Up to NNLO, the integration of the azimuthal angle of x_{T} commutes to the right of the beam and hard functions, and acts only on the soft function [17]. Remarkably, at each order in α_{s}, such azimuthal integration can be used to factor away the q'_{T} dependence[2]. We illustrate all this in Fig. 1.

Before the soft function can be evaluated, it is necessary to note that its individual contributions suffer from the so-called rapidity divergences associated to states that scale as $(\lambda^{\pm 1}, \lambda^{\mp 1}, 1)$. Non-trivially, the rapidity divergences at NNLO can be regularised by means of the analytic regulator [17, 20], *i.e.* by changing the integration measure as

$$\mathrm{d}^{4-2\epsilon}k_i\delta^+\left(k_i^2\right) \to \mathrm{d}^{4-2\epsilon}k_i\delta^+\left(k_i^2\right)\left(k_i^+\right)^{-\alpha}\ , \quad (6)$$

where α is a regulator analogous to ϵ in the dimensional regularisation. Upon integration, the different graphs that contribute to the soft function can be

[2] Hence, the integrations in the momentum and in the coordinates spaces can be easily related to each other.

$$\int \mathrm{d}\phi\, \boldsymbol{S}(\vec{q}_T, \vec{v}_t, \mu) =$$

$$\sum_{X_s} f_{X_s}(\vec{q}\,'_T) \int_{X_s} \delta\left(1 - \left|\textstyle\sum_i \vec{k}_{iT}\right|^2\right) \prod_i \delta^+(k_i)$$

$$= f_1(q'_T) \int \mathrm{d}^d k_1 \; \delta\left(1 - \vec{k}^2_{1T}\right)\delta^+(k_1)$$

$$+ f_2(q'_T) \int \mathrm{d}^d k_1 \; \delta\left(1 - |\vec{k}_{1T} + \vec{k}_{2T}|^2\right)\delta^+(k_1)\delta^+(k_2) + \ldots$$

Fig. 1. The azimuthally averaged soft function in the momentum space. The sum over X_s runs over all graphs that couple to the hard sub-process in the eikonal approximation, but with exact QCD interactions inside the hatched blob. The sum and product over k_i runs over the cut (on-shell) emissions. As explained in the main text, the dependence on q'_{T} has been factored out of the integration and is encoded by simple functions denoted by $f_a(q'_{\mathrm{T}})$. The bottom rows illustrate particular graphs that contribute, respectively, at NLO and at NNLO.

expanded both in α and ϵ. The α poles should be cancelled order-by-order in α_{s} and the ϵ poles should be cancelled by the SCET renormalisation procedure, see below.

The graphs that appear in the evaluation of the soft function are not standard due to the presence of the delta function that constraints the $k_{i\mathrm{T}}$ of the on-shell emissions, see Fig. 1. At NNLO, the soft function receives contributions from double-cut (double-real) and single-cut (mixed real-virtual) graphs. The virtual loop in the latter can be integrated out using the results of Ref. [21]. Due to this, below, we will focus on the double-cut graphs.

To integrate all the double-cut graphs, we have designed and automated an algorithm to numerically integrate these. Non-trivially, this is possible because double-cut graphs share a common structure that can be exploited. The backbones of this algorithm are:

1. Identify all the divergences of every contribution G to the soft function and separate its integrand as

$$G = \int \mathrm{d}^d k_1 \mathrm{d}^d k_2 \frac{\delta^+(k_1)\delta^+(k_2)}{\left(k_1^+ k_2^+\right)^\alpha} \delta\left(1 - |k_{1\perp} + k_{2\perp}|^2\right) \mathcal{I}_G \times \mathcal{W}_G \,, \quad (7)$$

where the defining property of the weight part $\mathcal{W}_G$ is that it has at most integrable singularities. In contrast, the infrared part $\mathcal{I}_G$ has divergences that, broadly speaking, gives rise to α and ϵ poles.

2. Map the integration variables $\{k_i\} \to \{x_{ij}\}$ to a minimal number of domains j, each of which is a unit hypercube ($x_{ij} \in [0,1]$) with singularities located only at zero.

3. Implement sector decomposition to disentangle and factorise the α and ϵ poles of each graph. The entire sector decomposition procedure depends only on the details of $\mathcal{I}_G$, and $\mathcal{W}_G$ is treated as a weight function. This is crucial for efficiency reasons. After this point, α and ϵ expansion renders expressions of the form of

$$G = \sum_j \sum_{r=-2, s=-3} \frac{1}{\alpha^r \epsilon^s} \int_{[0,1]^n} \mathrm{d}^n \vec{x} \; \mathcal{F}_{rsj}\left(\vec{x}, \theta, \beta\right) \,, \quad (8)$$

where now each integral on the right-hand side is finite.

4. In general, such integrals are intricate but we have found that these are suitable for a numerical evaluation using the CUBA library [22].

4. Validation of the integration strategy

In this section, we will describe a series of tests of our numerical integration. Let us start by noting that the only graphs that are proportional to the number of light quark flavours, n_f, are those that involve emission of a fermion pair. Due to this, the cancellation of poles should occur independently for this set of graphs. To check this, let us denote by G_{ij}^fer the graph in the third line of Fig. 1. Only the contributions with (i,j) set to $\{(1,t),(2,t),(1,\bar{t}\,),(2,\bar{t}\,)(t,\bar{t}\,),(t,t),(\bar{t},\bar{t}\,)\}$ are non-vanishing.

Both numerically and analytically, we have been able to compute all the poles of these graphs. Although, at intermediate steps, most integrals exhibit α poles, the only graphs that have these poles are

$$\begin{aligned} G_{1t}^\mathrm{fer} &= n_\mathrm{f} \boldsymbol{T}_1 \cdot \boldsymbol{T}_t \left(\frac{c}{\alpha} + \ldots\right) , \qquad G_{2t}^\mathrm{fer} = -n_\mathrm{f} \boldsymbol{T}_2 \cdot \boldsymbol{T}_t \left(\frac{c}{\alpha} + \ldots\right) , \\ G_{1\bar{t}}^\mathrm{fer} &= n_\mathrm{f} \boldsymbol{T}_1 \cdot \boldsymbol{T}_{\bar{t}} \left(\frac{c}{\alpha} + \ldots\right) , \qquad G_{2\bar{t}}^\mathrm{fer} = -n_\mathrm{f} \boldsymbol{T}_2 \cdot \boldsymbol{T}_{\bar{t}} \left(\frac{c}{\alpha} + \ldots\right) . \end{aligned} \quad (9)$$

By using colour conservation, one can show that the poles cancel when these graphs are added together. Indeed, this is what we find after combining all graphs

$$\begin{aligned} c(\text{analytically}) &= -\frac{8}{3\alpha\epsilon} - \frac{8(3\gamma_E + 5 - 3\log(2))}{9\alpha}\,, \\ c(\text{numerically}) &= -\frac{2.66}{\alpha\epsilon} - \frac{4.13}{\alpha} + \mathcal{O}\left(10^{-3}\right)\,. \end{aligned} \tag{10}$$

After the cancellation of the α poles, the ϵ poles of the bare soft function must be cancelled by the SCET renormalisation procedure [23]

$$\boldsymbol{S}(\mu) = \boldsymbol{Z}_s^{\dagger}(\mu,\epsilon)\boldsymbol{S}_{\text{bare}}(\epsilon)\boldsymbol{Z}_s(\mu,\epsilon)\,. \tag{11}$$

Again, we have singled out all contributions proportional to $n_{\text{f}}\alpha_{\text{s}}^2$ and confirmed that the $\boldsymbol{Z}_s(\mu,\epsilon)$ operators remove all the ϵ poles of graphs involving the radiation of a fermion pair.

Within our numerical approach, the graphs involving fermions are the most complicated. In spite of this, by means of ordinary differential equations, we have been able to solve analytically such contributions up to the order of $\epsilon^0\alpha^0$. Figure 2 shows the agreement between our numerical and analytic calculations for a particular combination of graphs. Analogous plots for other graphs can be found in [24]. This agreement holds with absolute accuracy of the order of 10^{-3}, which is the preliminary setting we used for the validation stage.

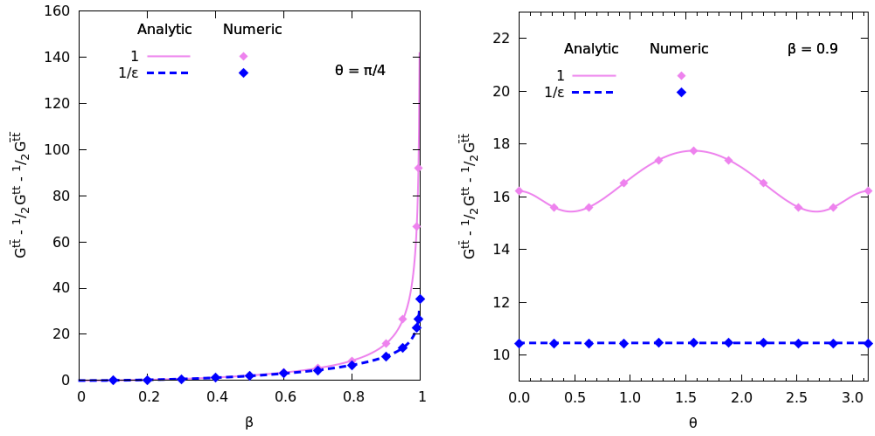


Fig. 2. The numerical and the analytic calculation of the kinematical part of $G_{t\bar{t}}^{\text{fer}} - G_{tt}^{\text{fer}}/2 - G_{\bar{t}\bar{t}}^{\text{fer}}$. Up to a global power of q_{T}', the soft function depends only on the velocity β and the polar angle, θ, of p_t.

5. Conclusions

Top-pair cross sections at NNLO can be evaluated by combining the slicing method and SCET. The only missing result to apply this is the SCET soft function at NNLO and we have developed an algorithm, based on the sector decomposition, to evaluate all of its contributions. To validate this algorithm, we focused on the part of the cross section proportional to $\alpha_s^2 n_f$ and showed that the rapidity and the infrared singularities cancel accordingly. Finally, by using ordinary differential equations, we also evaluated this part of the cross section analytically and found a perfect agreement with the numerical results, from our sector decomposition based algorithm. Therefore, we conclude that the study presented in this proceedings constitutes a proof of concept of an approach that can be generalised to other processes at high orders.

We thank Mateusz Dobija for helping us to optimise our implementation of the CUBA library. The project has received funding from the European Union's Horizon 2020 research and innovation programme under the Marie Skłodowska-Curie grant agreement No. 665778.

REFERENCES

[1] M. Czakon, *Nucl. Part. Phys. Proc.* **261–262**, 115 (2015).

[2] M. Czakon, P. Fiedler, A. Mitov, *Phys. Rev. Lett.* **110**, 252004 (2013) [arXiv:1303.6254 [hep-ph]].

[3] M. Czakon *et al.*, arXiv:1705.04105 [hep-ph].

[4] M. Czakon, D. Heymes, A. Mitov, *Phys. Rev. Lett.* **116**, 082003 (2016) [arXiv:1511.00549 [hep-ph]].

[5] G. Abelof, A. Gehrmann-De Ridder, I. Majer, *J. High Energy Phys.* **1512**, 074 (2015) [arXiv:1506.04037 [hep-ph]].

[6] G. Abelof, A. Gehrmann-De Ridder, *J. High Energy Phys.* **1412**, 076 (2014) [arXiv:1409.3148 [hep-ph]].

[7] R. Bonciani *et al.*, *Eur. Phys. J. C* **75**, 581 (2015) [arXiv:1508.03585 [hep-ph]].

[8] V. Ahrens *et al.*, *J. High Energy Phys.* **1009**, 097 (2010) [arXiv:1003.5827 [hep-ph]].

[9] V. Ahrens *et al.*, *J. High Energy Phys.* **1109**, 070 (2011) [arXiv:1103.0550 [hep-ph]].

[10] N. Kidonakis, *Phys. Part. Nucl.* **45**, 714 (2014) [arXiv:1210.7813 [hep-ph]].

[11] N. Kidonakis, *Phys. Rev. D* **91**, 031501 (2015) [arXiv:1411.2633 [hep-ph]].

[12] J. Gao, C.S. Li, H.X. Zhu, *Phys. Rev. Lett.* **110**, 042001 (2013) [arXiv:1210.2808 [hep-ph]].

[13] M. Brucherseifer, F. Caola, K. Melnikov, *J. High Energy Phys.* **1304**, 059 (2013) [arXiv:1301.7133 [hep-ph]].

[14] S. Catani, M. Grazzini, *Phys. Rev. Lett.* **98**, 222002 (2007) [arXiv:hep-ph/0703012].

[15] S. Dittmaier, P. Uwer, S. Weinzierl, *Phys. Rev. Lett.* **98**, 262002 (2007) [arXiv:hep-ph/0703120].

[16] S. Dittmaier, P. Uwer, S. Weinzierl, *Eur. Phys. J. C* **59**, 625 (2009) [arXiv:0810.0452 [hep-ph]].

[17] H.T. Li *et al.*, *Phys. Rev. D* **88**, 074004 (2013) [arXiv:1307.2464 [hep-ph]].

[18] T. Gehrmann, T. Luebbert, L.L. Yang, *J. High Energy Phys.* **1406**, 155 (2014) [arXiv:1403.6451 [hep-ph]].

[19] T. Gehrmann, T. Lubbert, L.L. Yang, *Phys. Rev. Lett.* **109**, 242003 (2012) [arXiv:1209.0682 [hep-ph]].

[20] T. Becher, G. Bell, *Phys. Lett. B* **713**, 41 (2012) [arXiv:1112.3907 [hep-ph]].

[21] I. Bierenbaum, M. Czakon, A. Mitov, *Nucl. Phys. B* **856**, 228 (2012) [arXiv:1107.4384 [hep-ph]].

[22] T. Hahn, *Comput. Phys. Commun.* **168**, 78 (2005) [arXiv:hep-ph/0404043].

[23] H.X. Zhu *et al.*, *Phys. Rev. Lett.* **110**, 082001 (2013) [arXiv:1208.5774 [hep-ph]].

[24] S. Sapeta, Proceedings of the 13$^{\text{th}}$ International Symposium on Radiative Corrections (RADCOR), PoS 2017.